In situ saxs characterization of thermoresponsive behavior of a poly(ethylene glycol)-graft-(poly(vinyl caprolactam)-co-poly(vinyl acetate)) amphiphilic graft copolymer

IOP Publishing Nanotechnology
Nanotechnology 34 (2023) 125602 (12pp) https://doi.org/10.1088/1361-6528/acab6d

In situ saxs characterization of thermoresponsive behavior of a poly (ethylene glycol)-graft-(poly(vinyl caprolactam)-co-poly(vinyl acetate)) amphiphilic graft copolymer

Mitchell A Kennedy[1], Yugang Zhang[2] and Surita R Bhatia[1,*]

[1] Department of Chemistry, Stony Brook University, Stony Brook, NY 11794-3400, United States of America
[2] National Synchrotron Light Source II, Brookhaven National Laboratory, Upton, NY 11973, United States of America

E-mail: surita.bhatia@stonybrook.edu

Received 14 June 2022, revised 6 December 2022
Accepted for publication 13 December 2022
Published 13 January 2023

Abstract

We report the thermoresponsive assembly and rheology of an amphiphilic thermosensitive graft copolymer, poly(ethylene glycol)-graft-(poly(vinyl caprolactam)-*co*-poly(vinyl acetate)) (commercial name Soluplus®), which has been investigated for potential biomedical applications. It has received attention due to is ability to solubilize hydrophobic drugs and for its thickening behavior close to body temperature. Through use of the synchrotron at Brookhaven National Lab, and collaboration with the department of energy, the nanoscale structure and properties can be probed in greater detail. Soluplus® undergoes two structural changes as temperature is increased; the first, a concentration independent change where samples become turbid at 32 °C. Increasing the temperature further causes the formation of physically associated hydrogels. This sol-gel transition is concentration dependent and occurs at 32 °C for 40 wt% samples, and increases to 42 °C for 10 wt% samples. From variable temperature SAXS characterization micelles of 20–25 nm in radius can be seen and maintain their size and packing below 32 °C. A gradual increase in the aggregation of micelles corresponding to a thickening of the material is also observed. Close to and above the gelation temperature, micelles collapse and form a physically associated 3D network. A model is proposed to explain these physical effects, where the poly(vinyl caprolactam) group transitions from the hydrophilic corona at room temperature to the hydrophobic core as temperature is increased.

Supplementary material for this article is available online

Keywords: Soluplus®, thermoresponsive, rheology, drug delivery, SAXS, hydrogel

(Some figures may appear in colour only in the online journal)

1. Introduction

Hydrogels are a diverse class of materials that have numerous medicinal applications due to their unique properties. Hydrogels have a high water content, which is usually

* Author to whom any correspondence should be addressed.

compatible with cell media, are flexible and can molded into shapes or films, can be permeable to oxygen, and can loaded with drugs [1–4]. Because of these properties, hydrogels have received much attention and use as wound dressings, adhesives, antibacterial coatings, tissue scaffolds, and drug delivery systems. Additionally, these materials can be imparted with a stimuli response such as temperature or pH, which influences gelation or the release of drugs [5–7]. Amphiphilic block copolymers are materials which contain multiple distinct blocks of varying hydrophobicity [8]. They generally form micelles at very low concentrations in water and can form gels at higher concentrations [7, 9]. These micelles have a high loading capacity and good stability in aqueous media [8]. Additionally, when one of the blocks, is thermoresponsive, increased temperatures can cause gelation. This behavior allows for injectable hydrogels, that are liquids at room temperature, and gels at body temperature [3]. These materials can be loaded with drugs and can be injected precisely for minimally invasive, targeted drug release [10].

Poly(ethylene glycol)-graft-(poly(vinyl caprolactam)-*co*-poly(vinyl acetate)) (PEG(13%)-graft-(PVCL(57%)-PVAc (30%)), average MW of 90-140 kDa) is a commercially available graft copolymer known as Soluplus® [11, 12]. The PEG backbone is a hydrophilic block and grafted blocks of hydrophobic PVAc and thermoresponsive PVCL are present as side chains, with 1-2 side chains present per PEG backbone. PVAc-co-PVCL copolymers have been shown to form small micelles between 7 and 22 nm in aqueous solutions at low temperatures; however, these PVAc-co-PVCL copolymers often become insoluble at temperatures <29 °C [13.] The addition of a hydrophilic PEG backbone changes the thermoresponsive properties of these systems, offering a wider range of temperatures at which the copolymers are soluble in water, and resulting structural and rheological transitions that are closer to physiological temperatures. Soluplus® solutions also display a gelling behavior that is unlike other thermoresponsive polymers, as the gels are very weak at all temperatures and show strong fRequency-dependent viscoelastic moduli [14, 15].

Soluplus® has been primarily studied as a means to increase the solubility of poorly soluble drugs. This is most commonly done in the solid phase, with Soluplus® forming a solid dispersion with a drug that cannot dissolve in water [11]. Solid dispersions of Soluplus® can be delivered as tablets and can release drugs at a constant rate over a period of several hours [16]. More recently, research has been focused on Soluplus® gels and solutions owing to its very low critical micelle concentration, and high drug loading capacity [17, 18].

Aqueous solutions of Soluplus® undergo a thermoreversible transition between 33 °C and 45 °C, which is in part accompanied by the solution becoming turbid. The addition of salts, or a change in the pH have been shown to affect the viscosity and lower critical temperature (LCT) of these solutions [19]. Solutions of Soluplus® have shown the capability of solubilizing drugs with high efficiency, while remaining stable over a period of months. Studies have also shown that the use of Soluplus® as a drug delivery device can increase the availability of poorly soluble drugs and increase their lifetime in the bloodstream [18, 20, 21]. Some room temperature scattering has been performed to examine the micellization behavior of Soluplus®, showing that it forms micelles with a packed core and hydrophilic corona [17]. Understanding the change in the structural properties as the temperature is increased; however, is vital to understanding its potential uses and limitations as a drug delivery system.

Soluplus® as a material has only been studied in the last decade, and there is still much to learn about its physical properties, structure, and potential applications. The bulk of the characterization and drug delivery studies have been on Soluplus® in the solid state, while studies on the solution properties have been much more scarce. Small angle x-ray scattering (SAXS) is a powerful tool in elucidating the nanoscale structures of dynamic soft materials, which can provide insight into their physical properties [22, 23]. In collaboration with the Department of Energy and Brookhaven National Lab, SAXS studies at the NSLS-II allowed for a highly detailed analysis into this material. In the present study, a comprehensive characterization of pure Soluplus® solutions and gels is performed, with a focus on physical and structural changes that occur as the material is heated. The mechanical properties were tested via rheological measurements, and structural properties and thermoresponsive mechanisms were probed through the use of dynamic light scattering (DLS) and SAXS.

2. Experimental

2.1. Materials and reagents

Soluplus® hydrogels and solutions were formulated through dissolution of Soluplus® in distilled water. Samples were stirred until solid powder was suspended homogeneously in solution. These solutions were then placed in the refrigerator overnight to aid with dissolution. The optically transparent solutions were kept in the refrigerator until needed for testing, at which point they were removed and brought to room temperature.

2.2. Turbidity and UV/VIS measurements

Turbidity was tested using a Varian Cary 100 Bio UV/Vis Spectrometer with a temperature control block and a source changeover at 350 nm. The instrument was run in transmission and double beam mode and background subtracted with a distilled water sample. All samples and background were collected in quartz cells. By observing real-time transmission at 800 nm, it was determined that a minimum of 5 min is needed more samples to equilibrate at each new temperature.

2.3. Rheology

Rheology was performed using a TA Instruments ARG2 Rheometer. A 40 mm 2-degree cone and plate geometry was used, and the samples were enclosed in a solvent trap during testing to prevent evaporation. An amplitude sweep from 0.01

to 10 Pa at 10 rad s^{-1} was performed to identify the linear viscoelastic region of each sample prior to testing. A single measurement at 10 rad s^{-1} and 0.59 Pa was performed at each temperature. Samples were equilibrated for at least 5 min at each temperature prior to testing.

2.4. Dynamic light scattering

DLS was performed using a Brookhaven Instruments Nanobrook Omni DLS. The samples were brought to room temperature prior to testing. A temperature ramp from 25 °C to 50 °C was used with samples allowed to equilibrate at the testing temperature for 5 min Counts were performed for 100 seconds in triplicate, then the data was averaged at each size.

2.5. Small-angle x-ray scattering

Samples for SAXS were loaded into 1.0 mm glass thin-walled capillaries (Charles Supper, Westborough, MA). The *in situ* SAXS measurements were conducted at the Complex Materials Scattering (CMS, 11-BM) beamline of the National Synchrotron Light Source II (NSLS-II) at Brookhaven National Laboratory. The scattered data were collected using a beam energy of 13.5 keV and beam size of 200 × 200 um with a Pilatus 2M area detector (Dectris, Switzerland). The detector, consisting of 0.172 mm square pixels in a 1475 × 1679 array, was placed five meters downstream from the sample position. The collected 2D scattering patterns were reduced to 1D scattered intensity, $I(q)$, by taking the circular average. Here q is the magnitude of the scattering wave vector, $q = (4\pi/\lambda)\sin(\theta)$, where λ and 2θ are the wavelength of the incident x-ray beam (0.9184 Å for these experiments) and the scattering angle, respectively.

2.6. Model fitting

SAXS data sets were fit primary using the core–shell sphere model in SasVeiw [24]. Other models used include the sphere model, which is simpler version of the core–shell sphere, and a hard sphere structure factor. Equation 1 shows the general model. The intensity is measured as a function of q, the scattering vector. Spherical models contain terms for the background and scale, which are added to and multiplied by the structure factor. The spherical model (equation 2) contains the fitting parameters of scale, background, SLD, SLD solvent and radius. The scale represents the precise volume fraction of scatterers if the SLDs are known or is a factor which is multiplied by the intensity. The background is added to the intensity at all q. The two SLD parameters are the scattering length density of the scatterer and the solvent, whose difference is Δp. The radius is the radius of the scatterer. Polydispersity can be added to this model by adding a degree of distribution to the radius. In these models, a Gaussian distribution of thickness and radius was used when available to average sizes over a disperse population, the implementation of which can be found in the Sasveiw documentation for polydispersity [25]. The core–shell model (equation 3) adds two parameters onto the spherical model, the thickness, and the SLD for the thickness. In the scattering function, V_s and V_c are the volume of the particle and volume of the core respectively, r_s and r_c are the radius of the entire particle and the radius of the core respectively, p_c, p_s and p_{solv} are the SLD of the core, the shell, and the solvent [24] . In addition to polydisperse radii, the core–shell model also can include polydispersity in the thickness

$$I_{\text{sphere}}(q) = \frac{\text{scale}}{V} * F^2(q) + \text{Background} \tag{1}$$

$$F_{\text{Sphere}}(q) = 3V(\Delta p)\frac{\sin(qr) - qr(\cos(qr))}{(qr)^3} \tag{2}$$

$$F_{CS}(q) = \frac{3}{V_s}\left[V_c(\rho_c - \rho_s)\frac{\sin(qr_c) - qr_c(\cos(qr_c))}{(qr_c)^3} + V_s(\rho_s - \rho_{\text{solv}})\frac{\sin(qr_s) - qr_s(\cos(qr_s))}{(qr_s)^3}\right]. \tag{3}$$

3. Results and discussion

3.1. Visual characterization of solutions

The Soluplus® solutions are fairly transparent at room temperature and have a slightly blue tint (figure 1). Bubbles form easily when the solutions are disturbed. The concentration of the samples has a clear correlation to the viscosity. Lower concentration solutions (< 10 wt%) flow freely. Above 10 wt%, the solutions begin to thicken gradually, though they do not from free-standing gels at room temperature; even at 40 wt%. When the samples are heated, they become turbid. This transition is accompanied by a thickening of the sample. At 50 °C, samples above 10 wt% form free-standing sticky gels and are white and opaque. When cooled to room temperature, the Soluplus® solutions revert back to a clear flowing liquid, indicating that this transition is thermoreversible.

3.2. Turbidity by UV/vis

Visual analysis showed that samples become turbid between room temperature and 50 °C, so UV/vis spectroscopy was employed to determine at what temperature this occurs. In figure 2(a), the transmission spectrum from 200 nm to 800 nm for 10 wt% Soluplus® can be seen as the temperature is increased from 25 °C to 50 °C. Even at room temperature, the samples absorb strongly in the blue light wavelengths, and almost completely in the UV region. As the temperature is increased, the transmittance across the entire spectrum is also decreased. Figure 2(b) shows the transmittance at 600 nm for samples ranging from 1 wt% to 20 wt%. From this, it can be seen that samples (above 1 wt%) become turbid between 31 °C and 33 °C. Before the samples become turbid, the transmittance decreases slightly with increasing temperature. This effect could be due to some slight micelle expansion or due to small aggregates forming. After the samples become turbid, the transmittance remains near 0% upon further heating.

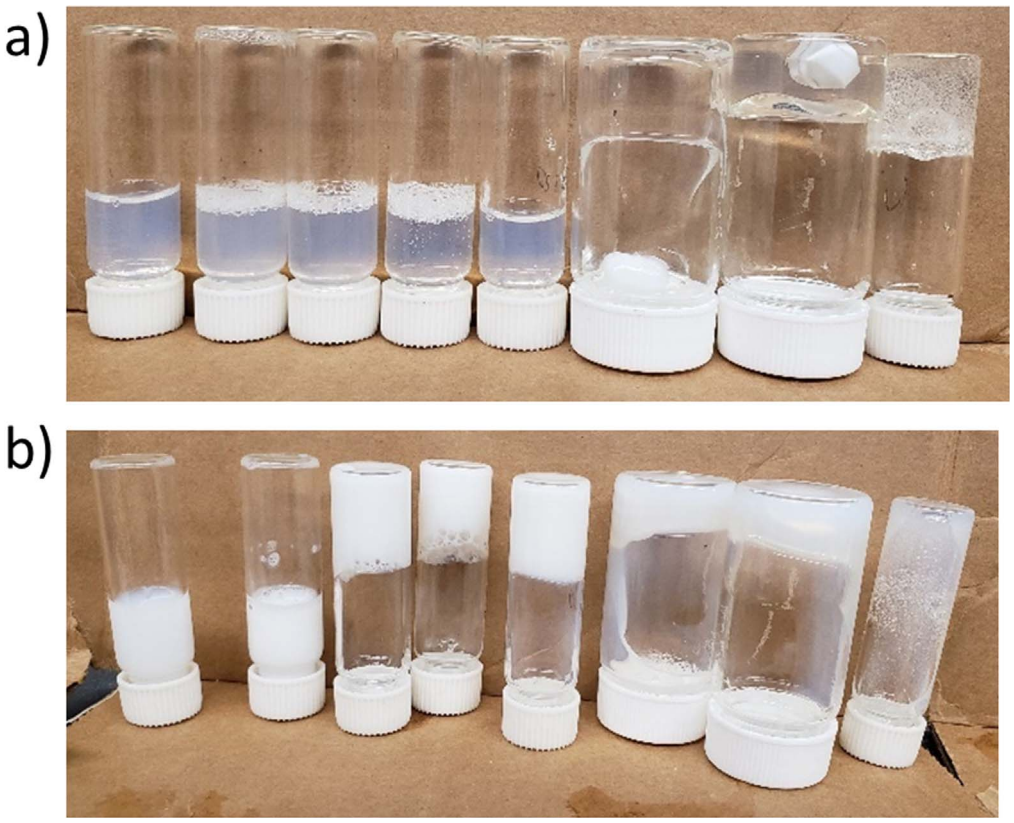

Figure 1. (a) Soluplus® solutions at room temperature. The solutions are arranged in increasing concentration (1, 5 ,10, 15, 20, 30, 35 and 40 wt%) from left to right. (b) Soluplus® solutions directly after being heated to 50 °C. The concentrations and arrangement are the same is in 1(a).

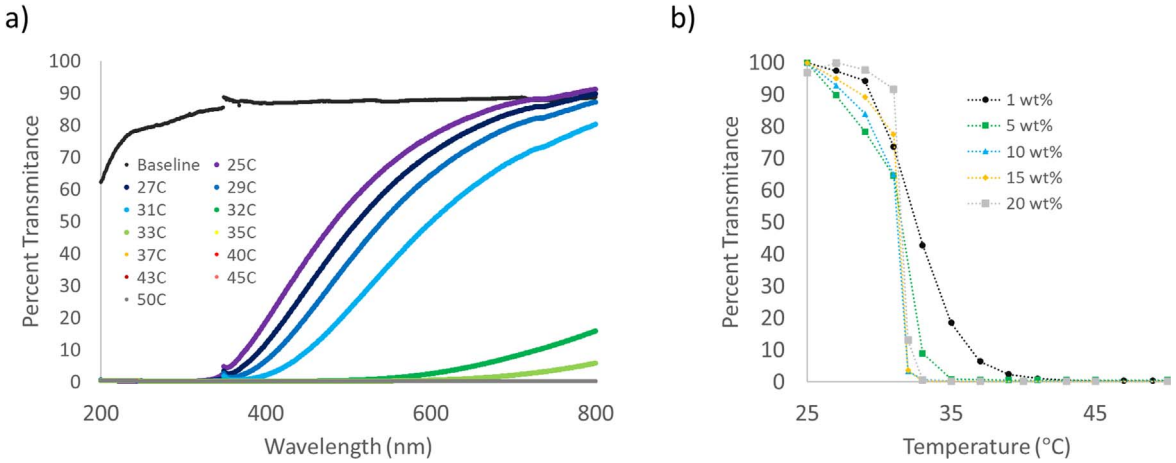

Figure 2. (a) The transmittance of 10 wt% Soluplus® solution ranging from 25 °C to 50 °C. Water (Baseline) was used at the background for these measurements. (b) Transmittance of Soluplus® solutions ranging from 1 wt% to 20 wt% at 600 nm. Samples were heated from 25 °C to 50 °C. The Resolution of the monochromator is 2 nm, while intensity was calibrated while measuring using a 2 beam mode.

3.3. Rheology of solutions

Rheological measurements of Soluplus® solutions (figure 3) were performed to further understand the mechanical change that accompanies the thermoresponsive behavior seen in the optical assessments. Single frequency measurements in the linear viscoelastic regime (LVR) were performed while increasing the temperature to assess viscoelastic changes that occur as the samples approach biologically-relevant temperatures. All of the solutions possess higher loss moduli at room temperature, indicating that the majority of force applied to the structures results in translation of the material. With lower concentrations (below 25%) the storage modulus is also too low to accurately measure, indicating the lack of any 3D structure. With the higher concentrations, both moduli are measurable and greatly increased, likely due to closer packing of micelles in solution.

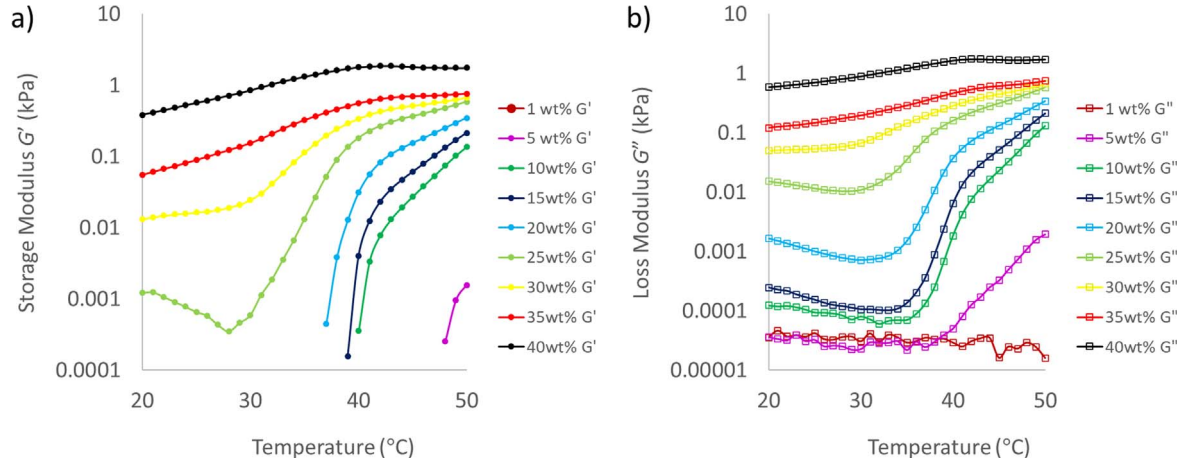

Figure 3. (a) The storage modulus (G') measured at each temperature from 25 °C to 50 °C of Soluplus® solutions ranging from 0.5 wt% to 40 wt%. Each measurement was taken in the LVR at 10 rad s^{-1}. (b) The loss modulus (G') measured at each temperature from 25 °C to 50 °C of Soluplus® solutions ranging from 0.5 wt% to 40 wt%. Each measurement was taken in the LVR at 10 rad s^{-1}. Error bars for Rheological measurements are not shown for clarity, but error in the measurements is typically between 1% and 5%. At lower moduli, close to the limits of the instrument, error can be higher (∼10%).

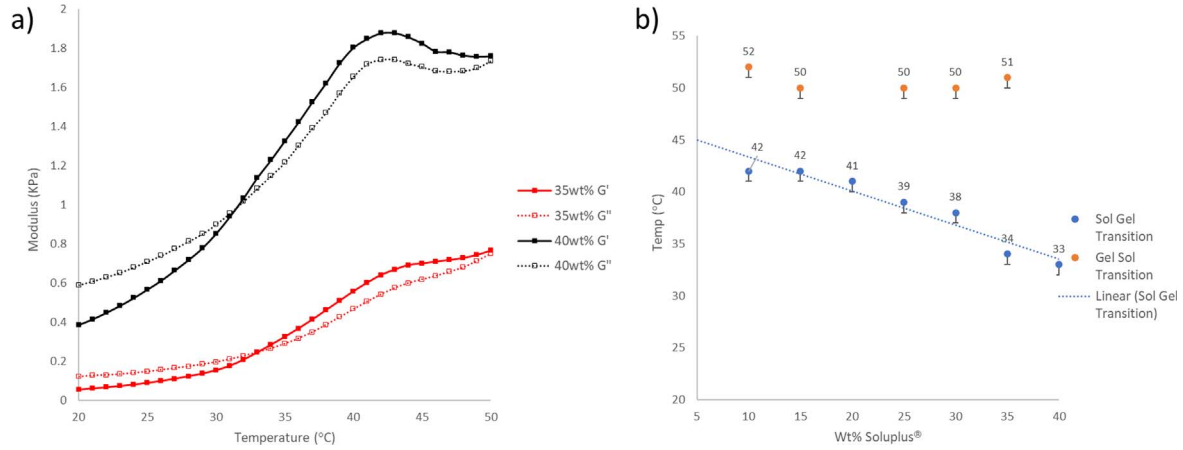

Figure 4. (a) Representative G'/G' plot as the temperature is increased for 20 wt% Soluplus®. The measurements were taken in the LVR at 10 rad s^{-1}. (b) representative G'/G' plot as the temperature is increased for 40 wt% Soluplus®. The measurements were taken in the LVR at 10 rad s^{-1}. (c) The sol-gel and gel-sol transition temperatures for Soluplus® solutions as the concentration is increased. Lower concentrations were omitted from this curve because they do not undergo a sol gel transition in this temperature range. The temperatures shown in (b) are the temperatures at which the transition has already occurred, where the transition occurs between temperatures.

When the temperature is increased, both the storage and loss moduli increase. Interestingly, though the solutions routinely become turbid between 31 °C and 33 °C, the change in the mechanical strength is more gradual and has some concentration dependence. The 1 wt% solution does not show any apparent change at this frequency as the temperature in increased. This is likely due to the dilute nature of the sample, where any structures present are too diffuse to absorb any applied force. The 5 wt% solution shows a similar behavior at lower temperatures, and does not begin to stiffen until 38 °C. Each of the other samples begin to stiffen and see a rapid increase to the storage modulus as temperature is increased. The loss modulus, however, decreases slightly as the temperature begins to increase. This effect is possibly due to the aggregation of small collections of micelles. From our turbidity measurements, we know that, at lower concentrations, small aggregates begin to form at 32 °C. This decrease in the loss modulus as gelation occurs has also been predicted to be a general feature for soft materials by some theoretical models; for example, the soft glassy rheology model of Sollich predicts a similar type of slight decrease in the loss modulus after an arrested state forms [26] due to these structures clumping to reduce the overall effective number of structures. The LCT, where a sol-gel transition exists, decreases semi-linearly with increasing concentration (figure 4). Above 5 wt%, a sol-gel transition occurs in the range of 33 °C–42 °C. For injectable purposes, transitions close to 37 °C are the most useful, making the solutions between 25 wt% and 35 wt% the most appropriate for this application.

The solutions begin to lose their elasticity as the temperature increases, which is shown by the continuous increase of the loss modulus and tapering of the storage modulus. Above 50 °C, the samples experience another critical point

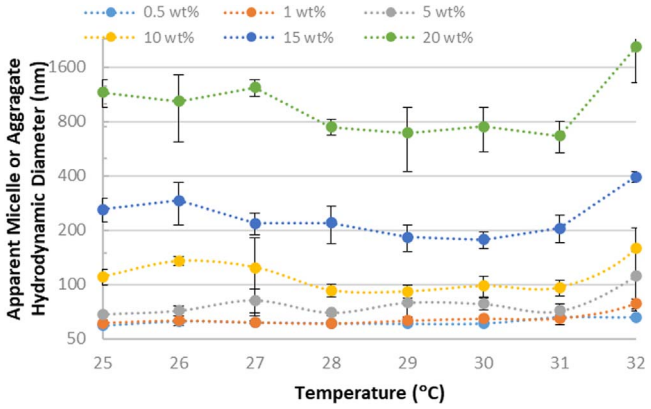

Figure 5. Mean apparent hydrodynamic diameter of particles present in Soluplus® solutions. Measurements were taken at each temperature from 25 °C to 35 °C for Soluplus® concentrations ranging from 0.5 wt% to 20 wt%. Data for concentrations $\leqslant$ 10 wt% represent diameters of individual micelles; the large increase seen for the 15 wt% and 20 wt% samples is due to formation of aggregates of micelles.

and melt routinely between 50 °C and 52 °C. Interestingly, the storage and loss moduli remain very close, even after the LCT, which could possibly indicate that, although a three-dimensional network structure may be present at these temperatures, it is physically associated and can be disturbed easily. This behavior could be favorable for applications as an injectable drug delivery system.

3.4. DLS characterization

To further examine the causes for the physical property changes in Soluplus® solutions, DLS was performed. DLS probes the hydrodynamic radius of particles in solution. Soluplus® is known to form micelles at very low concentrations in water at room temperature, which is a behavior consistent with other amphiphilic block copolymers [7, 9, 17]. At room temperature, the sizes of the micelles increase with the concentration of Soluplus® in solution. The two lowest concentrations, 0.5 wt% and 1 wt%, form micelles that are 59.4 $\pm$ 0.9 nm and 61 $\pm$ 2 nm in diameter, respectively. At higher concentrations these sizes increase to 69 $\pm$ 2 nm and 110 $\pm$ 10 nm for 5 wt% and 10 wt% solutions, respectively. The 15 wt% and 20 wt% samples have significantly larger apparent particle sizes at room temperature. The diameters DLS for the full series of concentrations and temperatures considered in this paper are shown in figure 5 and are tabulated in the Supplemental Information.

As discussed further below, SAXS does not show a dramatic increase in micelle size with concentration; thus, we believe that the apparent size increase that we see in DLS may indicate formation of aggregates of micelles. This also likely accounts for the increase in the storage moduli of these samples. As the temperature is increased, apparent particle sizes begin to increase slightly (figure 5). For the higher concentrations, there is a reduction of size around 27 °C before the particles start to follow the increasing trend. Around 32 °C, the samples become turbid. This transition temperature occurs more rapidly in the higher concentration samples, and there is a very large apparent increase in the particle size. It is important to note that DLS is generally not conducive for measurements on turbid samples, where multiple scattering can occur. This can lead to incorrect particle size measurements. Additionally, the Soluplus® samples begin to absorb very strongly in the visible region as they are heated, which can lead to artifacts in the particle size reading, as it uses a visible light laser. Despite this, it is predicted that the sample is becoming turbid due to aggregation of micelles into visible particles. This behavior continues as temperature increases which leads to formation of a three-dimensional network and gelation of the material.

3.5. SAXS

The SAXS data for Soluplus® solutions and gels (figure 6) shows a broad peak around 0.01 A^{-1} at higher concentrations. This peak likely corresponds to the micelle size, which can be seen in the DLS experiments. As the concentration of the solutions is increasing, the density of micelles in this size regime is also increasing. Interestingly, the size of the micelles does not change with concentration in the same fasion as the DLS data would suggest; in that it increases greatly with increasing concentration. The SAXS data instead shows that the radius of particles remains consistant, or increases slightly with increasing temperature. The micelles are not drastically increasing in size, but are actually agglomerating into larger structures, which can influence the DLS results.

Figure 7 shows representative fits for the 0.5 wt% and 20 wt% samples. At low concentration, there is no structure factor present in the scattering, and the experimental data conforms well to a spherical form factor. This data can also be modeled using a core–shell sphere form factor, although there is greater uncertainty in the parameters for the core–shell model as compared to the spherical form factor fit parameters. At these concentrations, there is no close-packing of micelles, and differentiating the core from the corona is difficult, contributing to the high uncertainty, while yielding very similar total radii as the spherical fit (supplementary information). With higher concentrations, the core–shell model is more robust, and an additional structure factor is needed. In this case, a hard sphere structure factor was used. As the temperature is increased, additional scattering of larger aggregates and eventually, the formation of a physically associated gel causes disagreement between a spherical form factor and the experimental data. It is likely that several different structures are contributing to the scattering at higher temperatures, reducing the robustness of a spherical fit.

The 1 wt% Soluplus® curves as the temperature increases can be seen in figure 8. At room temperature, the curve shows a spherical decay. Using the sphere model, the radius of the micelles can be estimated at 21 nm. This is slightly smaller than the values obtained from the DLS experiments (30 nm), which is common. DLS matures the hydrodynamic radius, where SAXS measures the radius of gyration. If the coronas are able to spread out and occupy more space in solution, this

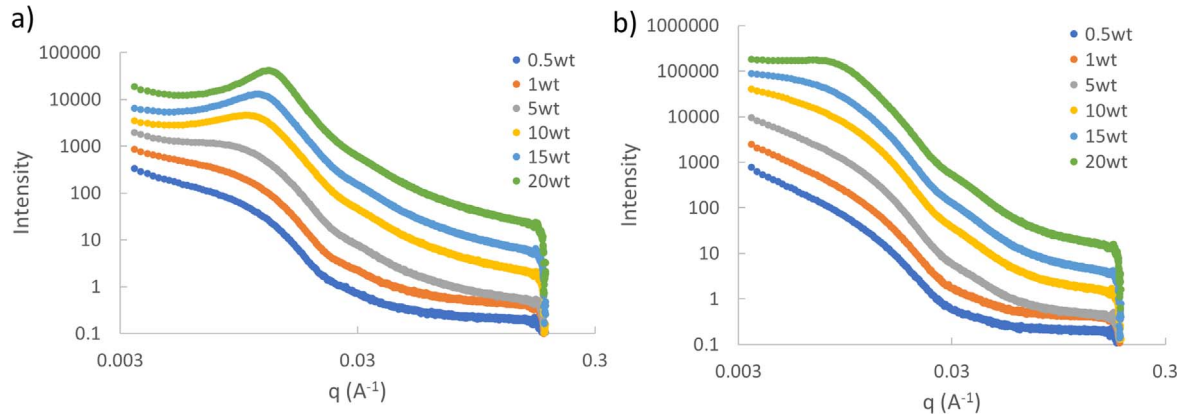

Figure 6. (a) SAXS measurements of Soluplus® solutions at 26 °C. Data have been vertically shifted by an arbitrary factor for clarity. (b) SAXS measurements of Soluplus® solutions at 50 °C. Data have been vertically shifted by an arbitrary factor for clarity.

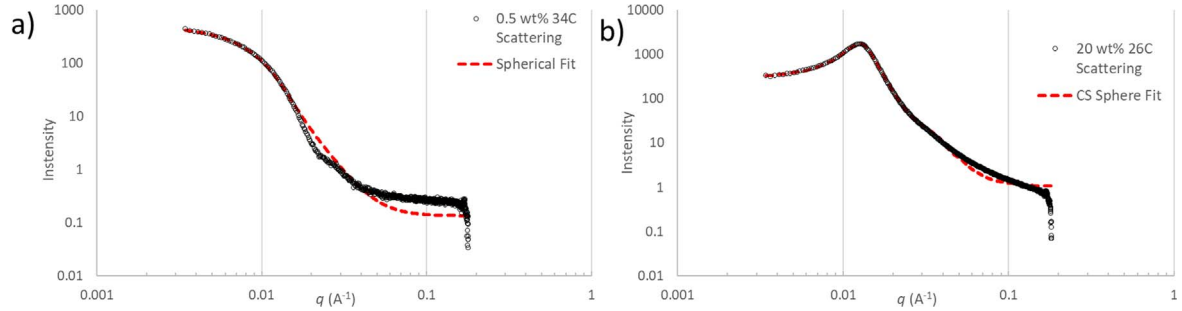

Figure 7. (a) Example fitting for 0.5 wt% Soluplus® at 34 °C. This fit used a spherical form factor with no structure factor. The fit parameters for the spherical form factor include a radius of 127 A^{-1}, and a polydispersity of 0.65. (b) Example fitting for 20 wt% Soluplus® at 26 °C. This fit used a core–shell sphere form factor with a hard sphere structure factor. The fit parameters for this form factor include a core radius of 157.5 A^{-1}, core polydispersity of 0.202, a corona thickness of 80.1 A^{-1}, corona polydispersity of 0 and a hard sphere radius calculated from the added radii of corona and core, and volume fraction 0.314. Additional fitting and parameters can be found in the Supplemental Information.

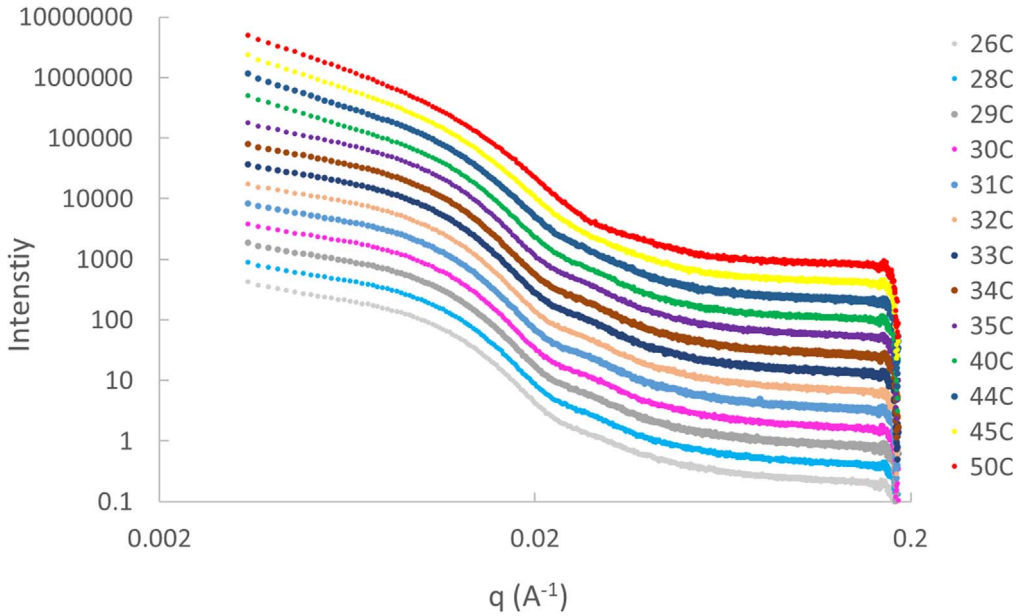

Figure 8. SAXS measurements of 1 wt% Soluplus®. Measurements were taken at 26, 28, 29, 30, 31, 32, 33, 34, 35, 40, 44, 45 and 50 °C. A smaller temperature increment was used between 30 °C and 35 °C because of the turbidity and rheological transitions observed in that region. Data have been vertically shifted for clarity.

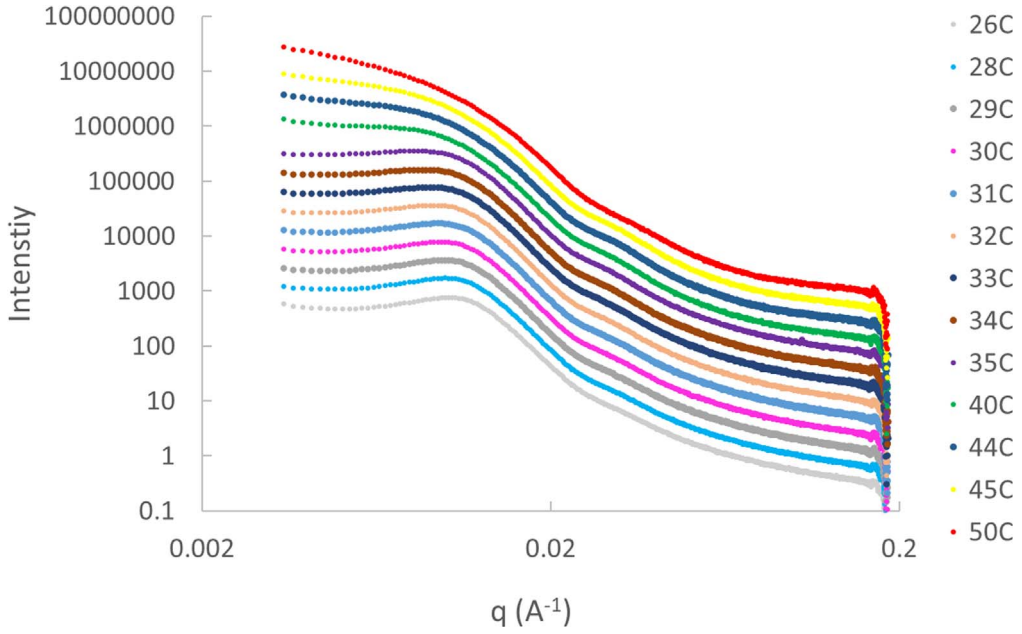

Figure 9. SAXS measurements of 10 wt% Soluplus®. Measurements were taken at 26, 28, 29, 30, 31, 32, 33, 34, 35, 40, 44, 45 and 50 °C. A smaller temperature increment was used between 30 °C and 35 °C because of the turbidity and rheological transitions observed in that region. Data have been vertically shifted for clarity.

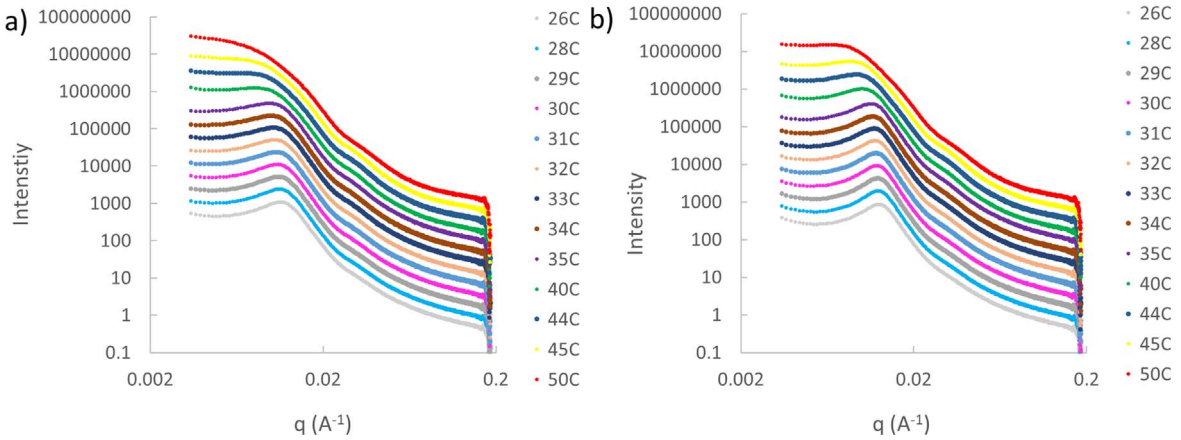

Figure 10. (a) SAXS measurements of 15 wt% Soluplus®. Measurements were taken at 26, 28, 29, 30, 31, 32, 33, 34, 35, 40, 44, 45 and 50 °C. A smaller temperature increment was used between 30 °C and 35 °C because of the turbidity and rheological transitions observed in that region. Data have been vertically shifted for clarity. (b) SAXS data for 20 wt% Soluplus®, taken in the same conditions as the 15 wt% Soluplus® solution. Samples from 0.5 wt% to 20 wt% were tested simultaneously in a single sample holder. Each data set has been shifted by an arbitrary factor to easier see differences in the data sets.

would lead to an increased size in DLS, but be less so registered in the SAXS data. As the temperature is increased, the feature around 0.01 A^{-1} is lost. Scattering at low q, cooresponding to the formation of larger structures washes out the micellar scattering at these higher temperatures. At this concentration, the micelle radius remains close to 21 nm up to 34 °C, where a sharp decline in size is observed. This is due to hydrophobic nature of the PVCL block at elevated temperature.

The 10 wt% Soluplus® scattering displays the same spherical decay, but a clear peak can be seen at room temperature (figure 9). The peak maximum corresponds to a micellar radius of 25.8 nm at room temperature and shifts to slightly lower q (larger size) as the temperature is increased. Again, by 50 °C, this feature becomes washed out by scattering at lower q. The scattering at high temperature is due to the scattering of aggregates, as well as individual micelles. This data can be modeled with the core–shell sphere with the addition of a hard sphere structure factor to encapsulate the feature around 0.1 A^{-1}.

Similar behavior can be observed in the higher concentration samples as in the 10 wt% sample (figure 10), although the peaks become more pronounced, as would be expected. The micelle sizes do not drastically increase, as the DLS results might suggest, and instead decrease slightly to 25.0 and 23.7 nm for 15 wt% and 20 wt% respectively. As the temperature is increased, the micelle sizes slightly increase before gelation occurs. At this temperature, the micelle sizes

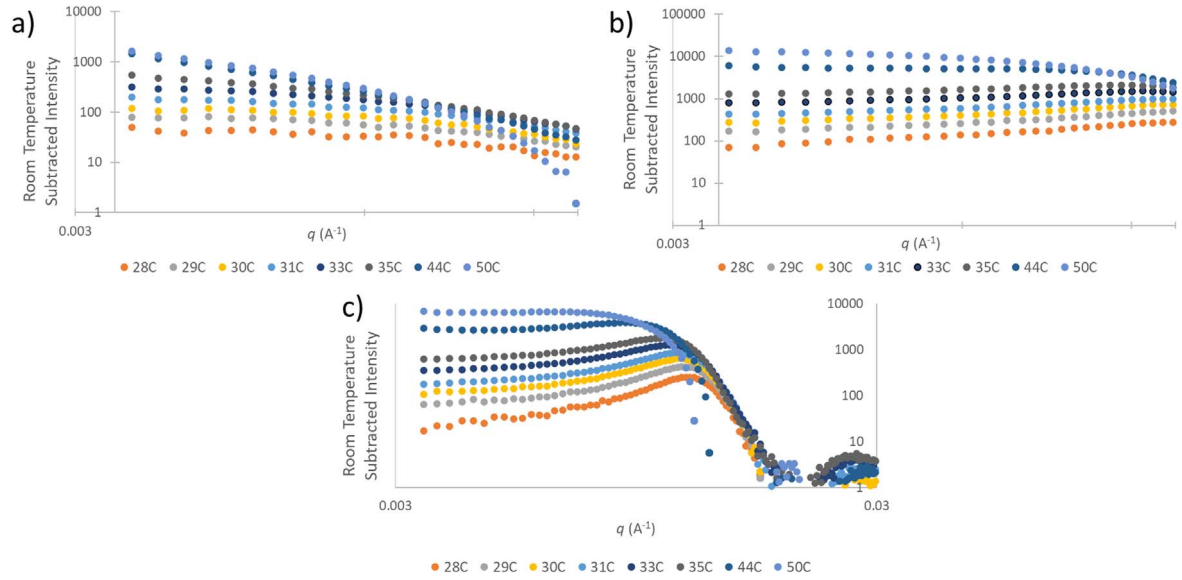

Figure 11. SAXS scattering of 1 wt% (a), 15 wt% (b) and 20 wt% (c) Soluplus® at selected temperatures with room temperature scattering subtracted. The 26 °C scattering was subtracted so that changes in scattering at low q can be identified.

tend to very greatly due the presence of multiple scattering structures present. Interestingly, though a visual change can be seen at 32 °C, from the aggregation of microscopic particles, no significant change in micelle size is observed. To further examine these temperatures, some additional treatments to the data were performed.

To further examine how the structures change as the temperature increases, aggregation behavior and the structure factor were isolated. The aggregation behavior can be elucidated by comparing the scattering at low q regions as the temperature is increased. To do this, the room temperature scattering intensity was subtracted from the scattering at each other temperature for a given sample. Figure 11 shows the plots of the low q region (0.003–0.01 A^{-1}), and a clear trend can be seen. As the temperature increases, the intensity of scattering in this region is increasing, and the slope is decreasing. This corresponds to the formation of larger structures in solution. The micelle size remains fairly consistent at lower temperature, below the gelation temperature; however, the aggregation shows a steady increase at all temperatures. This trend is reflected by the rheological study, which also showed a steady increase in the moduli as temperature is increased. This result implies that small micelles are aggregating into larger and larger clumps as the temperature increases.

The structure factor can be used to gain insight into how the micelles are arranged in solution, and how this packing changes with temperature. To highlight scattering arising from the structure factor, the total scattering for higher concentrations was divided by the scattering of a dilute solution; in this case, 0.5 wt% (figure 12). By dividing the dilute scattering, scattering resulting from the packing and interaction between particles in solution can be seen. At low temperatures, this structure factor is present and the result of hard sphere packing. The structure factor can be identified in this manor due to the high flux of synchrotron light sources. At 32 °C, the intensity of the structure factor remains consistent with room temperature, though it is shifted to slightly lower q (table of peak positions in supplementary). When temperature is increased further, the intensity of the structure factor as well as its position decreases drastically. In addition, the structure factor is broadened, indicating a range of particle or structure sizes interacting with each other at high temperature. This shows that the packing of particles, while well-defined at low temperatures, is reduced as larger structures form in solution. Some of the structure factor remains present at high temperature, indicating that micelles are likely still present, though they are fewer and more polydisperse.

3.6. Model discussion

By incorporating all of the data taken, a model can be proposed for the thermorevesable structural change of Soluplus®, depicted in figure 13. The structure can be thought of in three different states as the temperature is increased. At room temperature, Soluplus® forms micelles that are relatively well defined in size and shape. At this temperature, both the PEG and PVCL blocks are soluble in water and can form a core–shell spherical micelle with a hydrophylic, flexable corona containing these two blocks. The PVAc block forms a hydrophobic core that can be used to soluble drugs. When the temperature is increased, the PVCL blocks become less soluble and more preferentially orient in the core of the micelles, or closer to other micelles. This causes a gradual aggregation of small clumps of micelles. At 32 °C, aggregates become large enough that the samples become tubid. In this region, little change in the micelle size or packing is present. When the critical temperature is reached, the PVCL blocks are completely insoluble in solution, and the micelles aggregate into a much larger, pseudo 3-dimensional structure. This structure is likely large chains or groups of collapsed micelles which dynamically form short-lived physical cross-links with

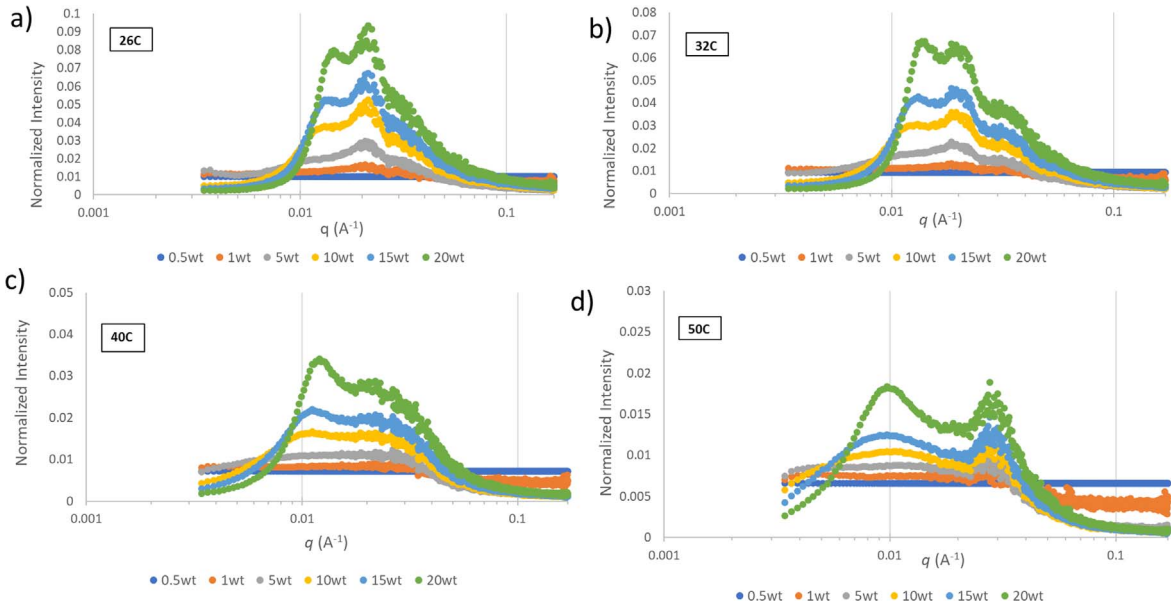

Figure 12. The scattering of Soluplus solutions with increasing concentration at (a) 26 °C, (b) 32 °C, (c) 40 °C and (d) 50 °C was divided by the scattering of 0.5 wt% Soluplus® to highlight scattering from the structure factor. The 0.5 wt% solution was assumed as a dilute solution containing a structure factor of 1 from particle-particle interactions in solution. Scattering at higher concentrations were divided by the dilute scattering so that only intensity due the particle packing or interactions are present. Each concentration was then normalized by dividing the scattering at each q from the total scattering of that sample over all q.

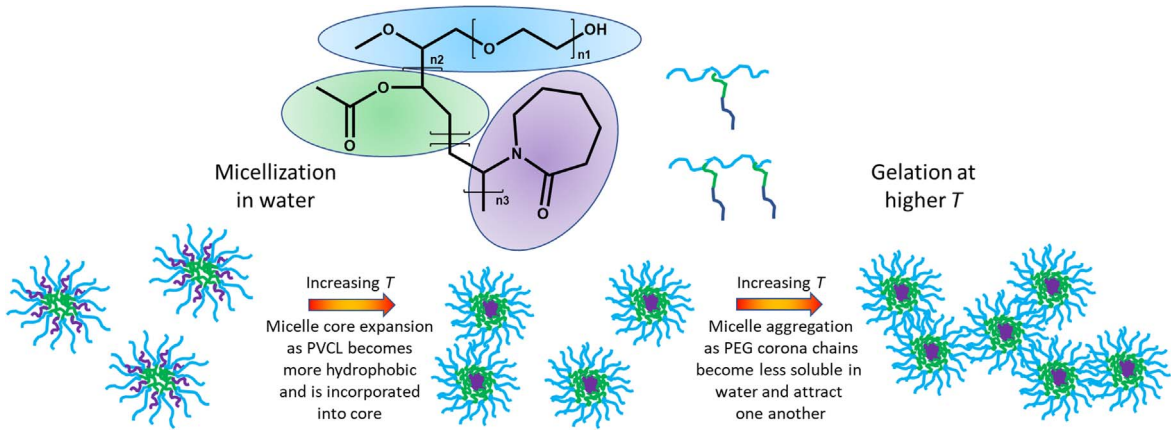

Figure 13. A representation of the proposed structural changes that occur in the Soluplus® solutions in relation to their thermoresponsive behavior. At room temperature, Soluplus® forms dispersed micelles or small micelle clusters. As the temperature is increased, the micelles begin to expand as the PVCL blocks become more hydrophobic. After the critical temperature, the PVCL blocks are no longer soluble in water and attractions between PEG blocks increase, and the structure becomes a weakly associated three-dimensional gel.

other chains. This change causes the samples to appear nominally solid-like. Higher frequencies of stress may disturb this structure, and cause breaking of the gel. Because the PEG blocks are still likely soluble in water, the structure is still quite soluble and does not percipitate out of solution.

4. Conclusions

Soluplus® is a promising candidate for a host of biomedical applications due to its unique properties. It has the capability to solubilize drugs that are highly permeable but difficult to deliver into the body as well as having thermosensitive properties. Soluplus® forms micelles in water at room temperature that are approximately 60 nm in diameter. The micelles have a hydrophilic corona and a hydrophobic core, which allows for hydrophobic drugs to be dissolved. As the concentration increases, the micelles are packed tighter in solution, which is shown by a perceived increase in diameter and a corresponding increase in the viscosity. As the temperature is increased, there exists a LCT, which is not concentration dependent, where the samples become turbid. It is proposed that the micelles are aggregating to form a larger network structure as the PVCL block becomes less soluble in solution. This aggregation continues after the samples become turbid, which causes a sol-gel transition in higher

concentration samples. This transition can be useful for applications as a drug delivery system, as the drug loaded micelles can be injected as a liquid and gel at body temperature.

It is important to understand the structural changes that occur in order to better design systems for drug delivery. Continued work can be done with this system in respect to how the drugs are encapsulated in the micelles, and their diffusion behavior at body temperatures. With this, the applications and limitations of Soluplus® for medicine can be better understood, and perhaps, even better drug delivery systems can be designed.

Acknowledgments

Support for MAK was provided by an NSF NRT award, DGE-1922639, and NSF DMR-1905547. This research used resources of the National Synchrotron Light Source II, U.S. Department of Energy (DOE) Office of Science User Facilities operated for the DOE Office of Science by Brookhaven National Laboratory under Contract No. DE-SC0012704. This work benefited from the use of the SasView application, originally developed under NSF award DMR-0520547. SasView also contains code developed with funding from the European Union's Horizon 2020 research and innovation programme under the SINE2020 project, grant agreement No 654000. The sponsoring agencies did not have any role in the study design; in the collection, analysis and interpretation of data; in the writing of the report; and in the decision to submit the paper for publication.

Data availability statement

The data that support the findings of this study are available upon reasonable request from the authors.

ORCID iDs

Surita R Bhatia https://orcid.org/0000-0002-5950-193X

References

[1] Liu S Q, Tay R, Khan M, Rachel Ee P L, Hedrick J L and Yang Y Y 2010 Synthetic hydrogels for controlled stem cell differentiation *Soft Matter* **6** 67–81

[2] Hiemstra C, Zhong Z Y, Jiang X, Hennink W E, Dijkstra P J and Feijen J 2006 PEG–PLLA and PEG–PDLA multiblock copolymers: synthesis and *in situ* hydrogel formation by stereocomplexation *J. Control. Release* **116** e17–9

[3] Kang Derwent J J and Mieler W F 2008 Thermoresponsive hydrogels as a new ocular drug delivery platform to the posterior segment of the eye *Trans. Am. Ophthalmol. Soc.* **106** 206–14

[4] Brandl F, Kastner F, Gschwind R M, Blunk T, Teßmar J and Göpferich A 2010 Hydrogel-based drug delivery systems: comparison of drug diffusivity and release kinetics *J. Control. Release* **142** 221–8

[5] Jeong B, Bae Y H, Lee D S and Kim S W 1997 Biodegradable block copolymers as injectable drug-delivery systems *Nature* **388** 860–2

[6] Khattak S F, Bhatia S R and Roberts S C 2005 Pluronic F127 as a cell encapsulation material: utilization of membrane-stabilizing agents *Tissue Eng.* **11** 974–83

[7] Wei L, Cai C, Lin J and Chen T 2009 Dual-drug delivery system based on hydrogel/micelle composites *Biomaterials* **30** 2606–13

[8] Kataoka K, Harada A and Nagasaki Y 2012 Block copolymer micelles for drug delivery: design, characterization and biological significance *Adv. Drug Deliv. Rev.* **64** 37–48

[9] Li J and Mooney D J 2016 Designing hydrogels for controlled drug delivery *Nat. Rev. Mater.* **1** 16071

[10] Norouzi M, Nazari B and Miller D W 2016 Injectable hydrogel-based drug delivery systems for local cancer therapy *Drug Discovery Today* **21** 1835–49

[11] Shamma R N and Basha M 2013 Soluplus®: a novel polymeric solubilizer for optimization of Carvedilol solid dispersions: formulation design and effect of method of preparation *Powder Technol.* **237** 406–14

[12] Bouillo N, Pierobon M, Widmaier R, Dobrawa R, Meyer-Boehm K and Lange R F-M 2012 *Use of copolymers as solubilizers for slightly water-soluble compounds* U.S. Patent 8,158,686

[13] Etchenausia L, Rodrigues A M, Harrisson S, Deniau Lejeune E and Save M 2016 RAFT copolymerization of vinyl acetate and N-Vinylcaprolactam: kinetics, control, copolymer composition, and thermoresponsive self-assembly *Macromolecules* **49** 6799–809

[14] Cespi M, Casettari L, Palmieri G F, Perinelli D R and Bonacucina G 2014 Rheological characterization of polyvinyl caprolactam–polyvinyl acetate–polyethylene glycol graft copolymer (Soluplus®) water dispersions *Colloid. Polym. Sci.* **292** 235–41

[15] Salah I, Shamat M A and Cook M T 2019 Soluplus solutions as thermothickening materials for topical drug delivery *J. Appl. Polym. Sci.* **136** 46915

[16] Linn M, Collnot E-M, Djuric D, Hempel K, Fabian E, Kolter K and Lehr C-M 2012 Soluplus® as an effective absorption enhancer of poorly soluble drugs *in vitro* and *in vivo Eur. J. Pharm. Sci.* **45** 336–43

[17] Mateos H, Gentile L, Murgia S, Colafemmina G, Collu M, Smets J and Palazzo G 2022 Understanding the self-assembly of the polymeric drug solubilizer Soluplus® *J. Colloid Interface Sci.* **611** 224–34

[18] Dian L, Yu E, Chen X, Wen X, Zhang Z, Qin L, Wang Q, Li G and Wu C 2014 Enhancing oral bioavailability of quercetin using novel soluplus polymeric micelles *Nanoscale Res. Lett.* **9** 684

[19] Hughey J R, Keen J M, Miller D A, Kolter K, Langley N and McGinity J W 2013 The use of inorganic salts to improve the dissolution characteristics of tablets containing Soluplus®-based solid dispersions *Eur. J. Pharm. Sci.* **48** 758–66

[20] Alvarez-Rivera F, Fernández-Villanueva D, Concheiro A and Alvarez-Lorenzo C 2016 α-Lipoic acid in soluplus® polymeric nanomicelles for ocular treatment of diabetes-associated corneal diseases *J. Pharm. Sci.* **105** 2855–63

[21] Varela-Garcia A, Concheiro A and Alvarez-Lorenzo C 2018 Soluplus micelles for acyclovir ocular delivery: Formulation and cornea and sclera permeability *Int. J. Pharm.* **552** 39–47

[22] Pape A C H, Bastings M M C, Kieltyka R E, Wyss H M, Voets I K, Meijer E W and Dankers P Y W 2014 Mesoscale

characterization of supramolecular transient networks using SAXS and Rheology *Int. J. Mol. Sci. [Online]* **15** 1096–111

[23] Kulkarni A R, Balaji R and Srinivasa R S 2010 Structural investigation of polyurethane based gel polymer electrolytes using small angle x-ray scattering (SAXS) *J. Phys. Soc. Jpn.* **79** Suppl 154–9

[24] Guinier A, Fournet G and Yudowitch K L 1955 *Small-Angle Scattering of X-rays* (New York: Wiley)

[25] Steve King P K 2021 Polydispersity & orientational distributions *SASVIEW Documentation.* www.sasview.org

[26] Sollich P 1998 Rheological constitutive equation for a model of soft glassy materials *Phys. Rev. E* **58** 738–59